

CONF-830805--33

DE83 010572

**HCDA Behavior Within the Primary Containment
of a Large Pool-Type LMFBR**

**W. R. Zeuch, C. Y. Wang, and R. W. Seidensticker
Reactor Analysis and Safety Division
Argonne National Laboratory
Argonne, Illinois 60439, U.S.A.**

The submitted manuscript has been authored
by a contractor of the U. S. Government
under contract No. W-31-109-ENG-3B.
Accordingly, the U. S. Government retains a
nonexclusive, royalty-free license to publish
or reproduce the published form of this
contribution, or allow others to do so, for
U. S. Government purposes.

DISCLAIMER

This report was prepared as an account of work sponsored by an agency of the United States Government. Neither the United States Government nor any agency thereof, nor any of their employees, makes any warranty, express or implied, or assumes any legal liability or responsibility for the accuracy, completeness, or usefulness of any information, apparatus, product, or process disclosed, or represents that its use would not infringe privately owned rights. Reference herein to any specific commercial product, process, or service by trade name, trademark, manufacturer, or otherwise does not necessarily constitute or imply its endorsement, recommendation, or favoring by the United States Government or any agency thereof. The views and opinions of authors expressed herein do not necessarily state or reflect those of the United States Government or any agency thereof.

MASTER

DISTRIBUTION OF THIS DOCUMENT IS UNLIMITED

fey

This paper discusses, specifically, the primary containment response of a large pool-type reactor under HCDA conditions. A large-diameter, thin-walled, pool-type reactor may have some inherent safety advantages in terms of energy accommodation during HCDA loads. The purpose of this study was to predict the containment response from the energetic excursion and to determine the impact loading on the reactor deck for a more detailed analysis. The essential features of the primary system which were modelled include the reactor core, radial shield, redan (separating the hot and cold pools), core support structure (CSS), upper internal structure (UIS), the sodium coolant, and the reactor vessel. Three different UIS configurations were studied and the effects of flow paths on the primary containment response were noted. In each case the primary systems were identical except for the upper internal structure (UIS) which was parametrically varied to simulate (1) annular flow, (2) a horizontal guide plate, and (3) a cylindrical shroud with guide plate.

The HCDA analysis and deck loading were obtained with the ALICE-II code (Arbitrary Lagrangian Implicit-Explicit Continuous-fluid Eulerian Code - second version). The specific advantages of using this code for the pool-type reactor design include the capabilities of modeling greatly distorted core bubble behavior, a curved reactor bottom, plates and perforations in the UIS, and internal thin shells which define the redan. An externally-generated HCDA source term was applied to the ALICE-II reactor model. The total energy of this source was 1000 MJ. Since the CSS was modelled as a rigid structure, most of the energy was transmitted upward as kinetic energy of the sodium.

The most significant result of the excursion analysis indicates that the energetics of the accident are contained within the redan, or hot pool region. Even though sodium was seen to spill over the redan into the cold pool, the sodium in this region remained virtually undisturbed. Maximum pressures of the sodium in the cold pool were about 0.5 MPa. The maximum radial displacement of the redan in the annular case was 15 cm, corresponding to 5.2% circumferential plastic strain.

The other two UIS designs both contain a guide plate which diverts the sodium flow in the radial direction. One case allowed all the sodium to be diverted radially. The other case modeled a perforated UIS shroud which limits the radial flow to about 20%. The increased radial flow caused 10.7% and 7.7% maximum redan strains in these two cases. However, the sodium outside the redan remained undisturbed.

1. Introduction

The advent of construction of commercial-sized liquid metal fast breeder reactor (LMFBR) plants has prompted the integrated primary system analysis of these large reactors. LMFBR reactor vessels range from about 12 to 22 m and contain liquid sodium at low pressure but high temperature. A large-diameter, thin-walled pool-type reactor design may have some inherent safety advantages in terms of energy accommodation during HCDA loads. The purpose of this study is to model several pool-type LMFBR designs under HCDA conditions and observe the primary containment response. This HCDA analysis is part of an integrated, full structural analysis of the primary system which also includes seismic response and detailed deck response to HCDA loads [1-2]. The calculations were made to establish overall feasibility of the conceptual designs with regard to acceptable vessel behavior under severe loadings from energetic releases within the vessel. Because much of the equipment is supported by the reactor vessel deck and triple rotating plug assembly, this support structure is given major emphasis in the analysis.

Figure 1 shows the overall primary system within the reactor vessel, including primary pumps, intermediate heat exchangers (IHXs), reactor core, core support structure (CSS), and a cylindrical internal vessel - called the redan - which separates the hot pool of sodium emerging from the top of the core from the cooler bulk sodium. Also shown are the triple rotating plugs in the deck, upper internal structure (UIS), and other components which are supported by and penetrate the deck structure.

Three separate designs were analyzed - the essential difference among them being the UIS configurations. The primary system in each of these designs is identical except for the UIS which was parametrically varied to simulate (1) annular flow, (2) a horizontal guide plate, and (3) a cylindrical shroud and guide plate.

2. HCDA Analysis

The HCDA analysis and deck loading were obtained with the ALICE-II code (Arbitrary Lagrangian Implicit-Explicit Continuous-fluid Eulerian Code - second version) [3-5]. ALICE-II uses a hybrid Eulerian-Lagrangian fluid mesh, treats the core-gas bubble in Eulerian coordinates, has two-dimensional axisymmetric shell elements, treats solids as elastic-plastic materials, calculates the fluid free surface based on the MAC-ICE technique, treats internal thin shells, handles perforated structures, incorporates a curved reactor vessel bottom, accommodates large, distorted bubble behavior, and has a three-dimensional treatment of movable upper internal structure. The specific advantages of using ALICE-II for the pool reactor design include capabilities of modeling greatly distorted core bubble behavior during the energy release, a curved reactor bottom, plates and perforations in the upper internal structure, and internal thin shells which define the redan.

A complex phenomenon, such as an energetic core energy release in a complex primary containment design, requires a most advanced analytical tool. ALICE-II is able to give a graphic representation of energetics accommodation by characterizing the energy release and the complex fluid-structure interaction in the containment interior.

2.1 Reactor Model - Annular UIS

The ALICE-II model of what shall be called the "reference" design is shown in Fig. 2. The essential features modeled include the reactor core, the sodium coolant, radial shielding, redan, UIS, reactor vessel wall, core-support structure, and the reactor cover. The upper internal structure (UIS) in this reference case is modeled as a right cylindrical

obstacle with a single annular flow channel of equivalent cross-sectional area as the actual perforated plate. The vertical annular opening extends through the entire length of the UIS. The redan is modeled as an internal, cylindrical, thin shell. A sodium free surface is maintained to model slug impact from vertically accelerated sodium impinging on the reactor cover. The force on the cover is determined as impact occurs. The reactor cover, consisting of a deck structure with a rotating plug assembly is modeled simply as a single piece, rigid body, capable of vertical motion, and secured by holdown bolts. The core support structure is modeled as a rigid structure at the bottom of the primary vessel. It was made rigid to provide a conservative slug impact loading on the reactor cover, since no energy can be attenuated in the negative axial direction.

The reactor core consists of a core-gas bubble with a specific equation-of-state in the form of a pressure-volume function (see Fig. 3). The equation-of-state for the core region was determined from a study of many core expansions generated by ramp reactivity insertions and from empirical fits of excursions in homogeneous and heterogeneous cores. Although Fig. 3 carries the expansion to 1 MPa, the actual equation-of-state continues to 0.1 MPa (1 atm) with a total expansion energy of 1000 MJ. Since there is finite room for expansion of the core-gas bubble within the primary containment, the total energy is not released, and a residual pressure exists as the system reaches dynamic equilibrium after the excursion. The available volume for expansion consists of the initial cover-gas volume plus the added volume due to the radial deformation of the reactor vessel and the upward motion of the reactor cover.

2.1.1 Results (Annular UIS)

Figure 4 gives a visualization of the core disruption and the containment response throughout the period of greatest core energy release in the system. At 112 ms after the initiation of the event the core bubble has begun to expand into the UIS and the first significant impact of sodium is seen on the underside of the rotatable plugs. It is important to note that the energy source in the core-gas bubble accelerates the sodium inside the UIS as well as the sodium between the UIS and redan. The presence of the UIS in separating the sodium flow results in slug impact with a slug which is no longer coherent. Peak forces are thereby reduced. Coolant is forced around and through the UIS as the core bubble expands, and there occurs some radial deformation of the core barrel and redan. Beginning even at 112 ms, there is noticeable deformation of the redan. The energy release is contained within the hot pool and strain energy is absorbed in the structure present there. By 208 ms the sodium has begun to spill over the top of the redan into the cold pool, but even at 360 ms, when the redan has reached its maximum plastic deformation, the sodium between the redan and primary vessel remains virtually undisturbed. The maximum radial displacement of the redan was 19 cm. This corresponds to a plastic strain of 5.2%. The maximum circumferential strain of the primary vessel was only 0.08%.

Figure 5 shows the force history of the reactor cover over the duration of the energy release for this reference case. This force history denotes the total fluid force on the cover at any particular time. Note that there are periods where there either is no contact of sodium on the cover, or the fluid is experiencing rarefaction and the force becomes zero. The first impacts of sodium from the hot pool inside the redan occur around 100 ms. Since the sodium was forced through several pathways along its vertical route to the cover, the loading appears as a series of sprays. As more sodium is accelerated and more energy is

released from the core a maximum force of 150 MN occurs at 190 ms. The maximum vertical displacement of the reactor cover was 0.18 cm, an insignificant amount. A large slug of sodium has been pushed out of the hot pool and is being forced over the redan (see Fig. 4). By 350 ms this slug has entered the cold pool region, the forces on the reactor cover have subsided, and the driving pressure of the core has dropped from its initial 23 MPa to 0.6 MPa. This corresponds to an energy release from the core of approximately 470 MJ.

2.2 Reactor Model - UIS Guide Plate

The ALICE-II model of the pool-type reactor with a horizontal guide plate in the UIS is shown in Fig. 6. All the essential features which were modeled in the reference annular case are identical except for the UIS. In this case the structure of the UIS is much farther from the core and has no axial flow paths. This model permits unrestricted expansion of the core-gas bubble until the guide plate is encountered, prohibiting all axial flow.

2.2.1 Results (UIS Guide Plate)

Reactor configurations at three different times during the excursion are shown in Fig. 7. At 112 ms after the initiation of the accident the sodium has begun to impact the head. In this case only a single flow path is available to the accelerated sodium - the annular space between the UIS and redan. It is possible to observe, from Fig. 7, the sodium motion as it is accelerated axially to contact the guide plate, then moves radially outward from the centerline, around the corner of the UIS, and toward the reactor cover.

Since the presence of the guide plate acts as a blockage to axial flow, the sodium has a smaller flow area, relative to the annular case, and the initial axial kinetic energy of the sodium must be transformed into radial kinetic energy. It is obvious, from Fig. 7, that this increases the stress on the redan. At 112 ms the redan has already reached its maximum radial deformation of 39 cm, corresponding to a plastic strain of 10.7%. As the redan is deformed near its midsection, the top edge is pulled downward, allowing more flow from the hot pool inside the redan to the cold pool outside. Again, the main body of fluid outside the redan is virtually undisturbed, and the maximum circumferential strain of the primary vessel was only 0.15%.

At 350 ms the core pressure is 0.8 MPa and approximately 380 MJ of the potential 1000 MJ has been released from the core. Since the driving pressure in the core is now very low and the available expansion volume within the primary system has been used, the system will reach dynamic equilibrium and the pressure waves will be damped out in the large pool of fluid.

2.3 Reactor Model - Guide Plate and UIS Shroud

The ALICE-II model of the pool-type reactor with a horizontal guide plate, a cylindrical UIS shroud, and a horizontal perforated plate is shown in Fig. 8. All the essential features which were modeled in the reference annular case are identical except for the UIS region. The complex flow paths in this modified design require the fluid moving through the UIS to flow in through a bottom perforated plate (50% perforation ratio) and out through a perforated cylindrical shroud (perforation ratio 20%). Again, axial flow through the UIS is restricted by the guide plate which blocks the direct vertical pathway to the reactor cover.

2.3.1 Results (Guide Plate and UIS Shroud)

Figures 9 and 10 show reactor configurations at five different times during the accident. This complex case was analyzed over a longer period than the previous two in order to observe the sodium after it spilled over the redan. At 112 ms after the initiation of the accident the sodium has impacted the underside of the reactor cover. The core-gas bubble by

this time has expanded into the UIS as well as around it. Radial flow through the cylindrical shroud is evident, as is the presence of trapped sodium just below the guide plate.

The presence of the UIS shroud acts as a partial blockage to radial flow and radial pressure wave propagation, as the guide plate acts as a complete blockage to upward axial flow and pressure propagation. The result is that the redan is partially shielded from the sodium pressure waves in the UIS region, especially those directed radially by the guide plate. At 112 ms the redan has already reached its maximum radial deformation of 26 cm, corresponding to a plastic strain of 7.7%. Sodium spills radially over the redan into the cold pool and this wave reaches the vessel wall at approximately 1 second. The sodium in the cold pool remains relatively undisturbed until the endpoint of the calculation, where numerical instabilities occur from the lengthy duration of the calculation and the large motion of the core-gas bubble and fluid particles. The maximum circumferential strain of the primary vessel was 0.13%. At 360 ms the core pressure was 0.86 MPa and approximately 360 MJ has been released from the core.

3. Comparisons and Conclusions

A summary of results for the three cases is shown in Table 1. The core-gas bubble in the annular model was confined least and, consequently, was able to expand more easily and release more energy than the other cases. Also, since there was freedom to expand axially, the redan strain was the lowest of the three cases. Of the two cases including the guide plate, the redan strain was much lower in the model containing the UIS shroud, since radial pressures were attenuated by this structure. The primary vessel strain behavior is in proportion with the redan strain, for the three cases, but at a magnitude which is insignificant. The redan, therefore, is a useful structural member for pressure attenuation as well as for separating the coolant pools.

Figures 11 and 12 show, respectively, comparisons of the core pressure histories and the core energy released from the three cases studied. Since the only difference in the three cases was the UIS configuration, certain conclusions can be drawn from the comparison of these data.

From the nature of the core-gas equation of state (see Fig. 3) the pressure in the core drops rapidly as the core-gas bubble begins to expand. By 100 ms, as shown in Fig. 11, the core pressure has dropped from 23 MPa to approximately 1.5 MPa in all three cases. By this time a large fraction of the energy has been imparted to the sodium coolant and much of the deformation of structures surrounding the core, including the redan, has been accomplished (see Figs. 4, 7, 9).

The difference in the pressure histories for the three cases in Fig. 11 can be explained by the degree of confinement of the core-gas bubble. The annular case allows the bubble to expand directly to the reactor cover and, therefore, expands at a higher rate. The other two cases are more confined having the vertical pathway through the UIS cut off. The extreme case of the UIS shroud, perforated bottom plate, and guide plate permits the slowest expansion. Perhaps a more meaningful interpretation can be given to this process by observing the energy released from the expanding core-gas bubble.

Figure 12 shows a comparison of the energy released from the core during these three excursions. Both the rate and the characteristics of energy release can be observed from this figure. Before 100 ms the three cases are quite similar. This would be expected since

he expanding bubble does not encounter the low-hanging upper internal structure in the annular or the shroud case until approximately 100 ms. After this time, however, there is a very marked influence on the rate of energy release.

The factor contributing most to reducing the rate of energy release from the core is the presence of the horizontal guide plate which prevents vertical flow of sodium to the cover region. In both cases where the guide plate is present the total energy released during the critical time of the accident is reduced, as is the rate of energy release. There is some additional mitigation of energy release due to the lower perforated plate and the UIS shroud in the third case, but this is minimal relative to the effect of the guide plate. In the reference case, with the annular pathway through the UIS, the sodium is continuously accelerated upward, releasing 100 MJ more energy from the core during this time period. Not only does the slug have a direct pathway through which it can impact the reactor cover, but the slug has more kinetic energy imparted to it. The complex model, including the guide plate and UIS shroud, exhibits the most desirable features for accident accommodation.

4. Acknowledgments

This work was performed in the Engineering Mechanics Program of the Reactor Analysis and Safety Division at Argonne National Laboratory, under the auspices of the U.S. Department of Energy.

References

- [1] SEIDENSTICKER, R. W., et al., "Scoping Calculations for Design and Analysis of Large Reactor Vessels for Liquid-Metal Fast Breeder Reactor (LMFBR) Plants," in Pressure Vessel Design, 1982 ASME Special Publication PVP-Vol. 57, pp. 141-154 (June, 1982).
- [2] KULAK, R. F., FIALA, C., PAN, Y. C., SEIDENSTICKER, R. W., "Structural Behavior of a Pool-Type LMFBR Reactor Vessel Deck to Beyond Design Basis Loads," Trans. 7th Int'l. Conf. on Structural Mechanics in Reactor Technology, paper E 1/9, Chicago, IL (August, 1983).
- [3] WANG, C. Y., ZEUCH, W. R., "ALICE-II: An Arbitrary Lagrangian-Eulerian Code for Containment Analysis with Complex Internals," Trans. Am. Nucl. Soc., Vol. 41, p. 364 (June, 1982).
- [4] WANG, C. Y., ZEUCH, W. R., "A Multi-Dimensional Arbitrary Lagrangian Eulerian Method for Dynamic Fluid-Structure Interaction," in Fluid-Transients and Fluid/Structure Interaction, eds., Y. W. Shin, F. J. Moody, M. F. Au-Yang, 1982 ASME Special Publication PVP-64, Book. No. H00221, pp. 289-316 (June, 1982).
- [5] WANG, C. Y., ZEUCH, W. R., "Recent Developments of the Arbitrary Lagrangian-Eulerian Containment Code ALICE-II," Trans. 7th Int'l. Conf. on Structural Mechanics in Reactor Technology, paper E 4/8, Chicago, IL (August, 1983).

Table I

<u>Reactor Model</u>	At 360 ms,		<u>Max. Redan Strain (%)</u>	<u>Max. Vessel Strain (%)</u>
	<u>Core Pressure (MPa)</u>	<u>Core Energy Released (MJ)</u>		
Annular UIS	0.59	469.	5.2	0.08
UIS Guide Plate	0.80	383.	10.7	0.15
Guide Plate and UIS Shroud	0.86	364.	7.7	0.13

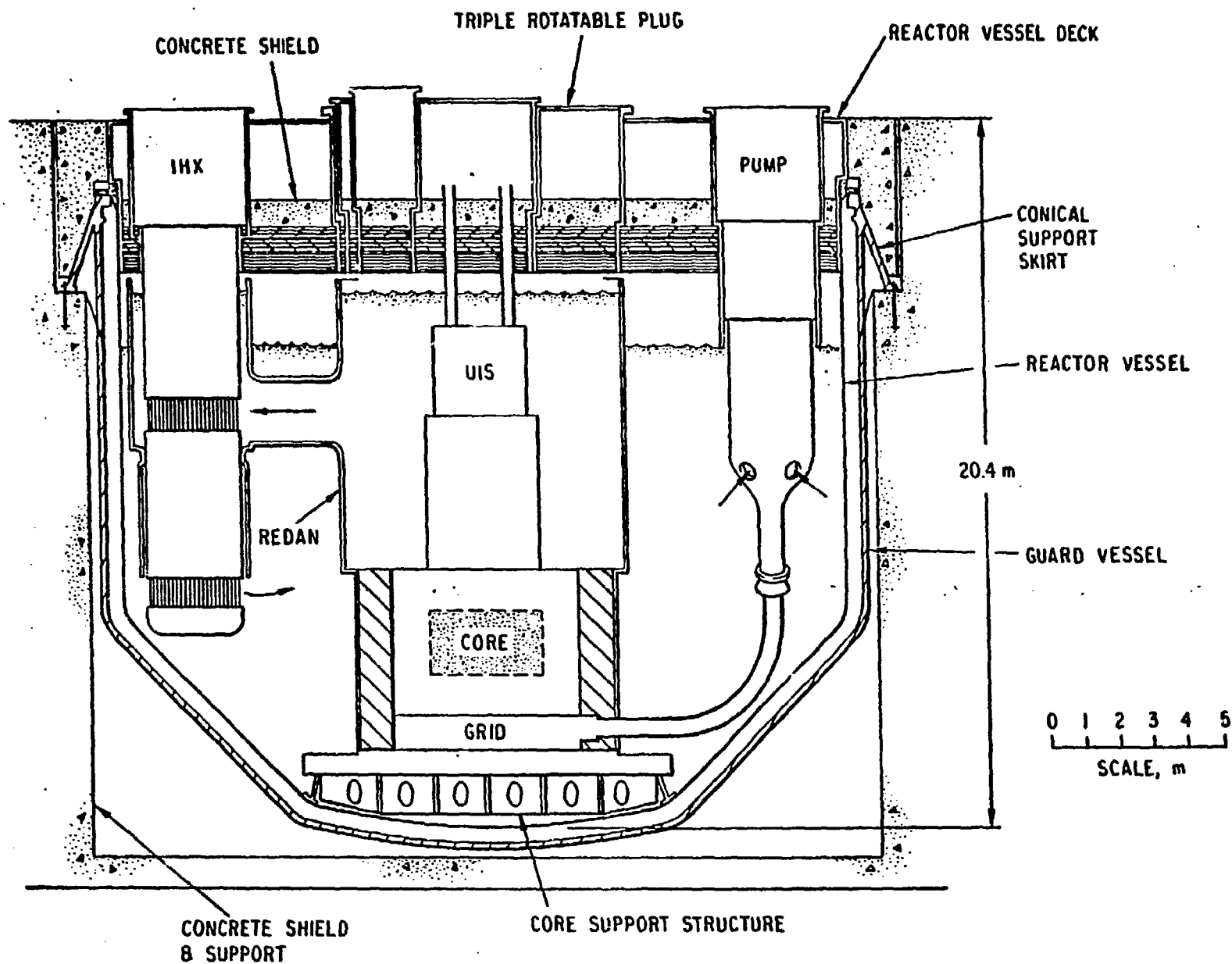


Fig. 1. Schematic of Pool Reactor Primary System

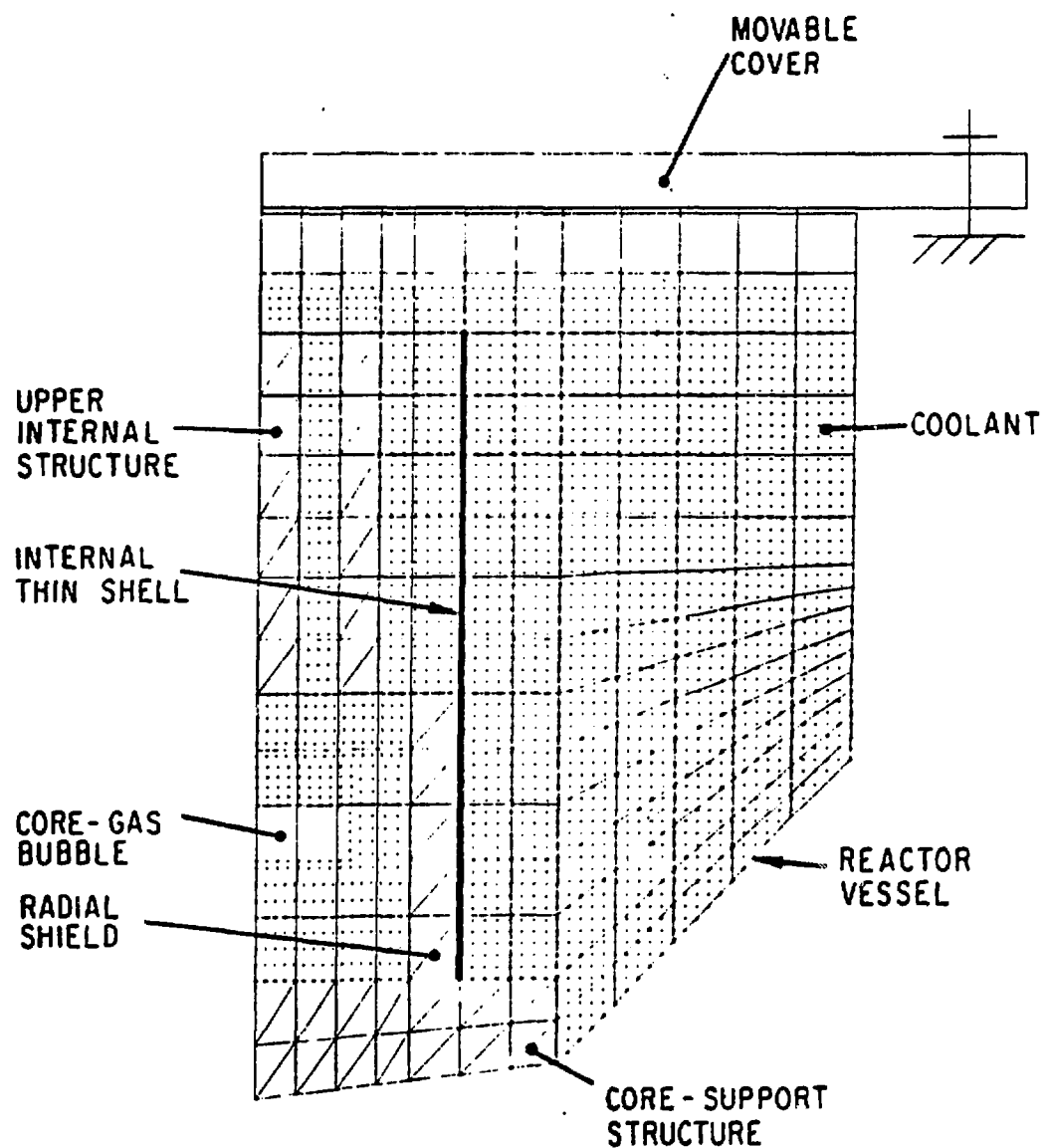


Fig. 2. ALICE-II Model of Pool Reactor with Annular UIS

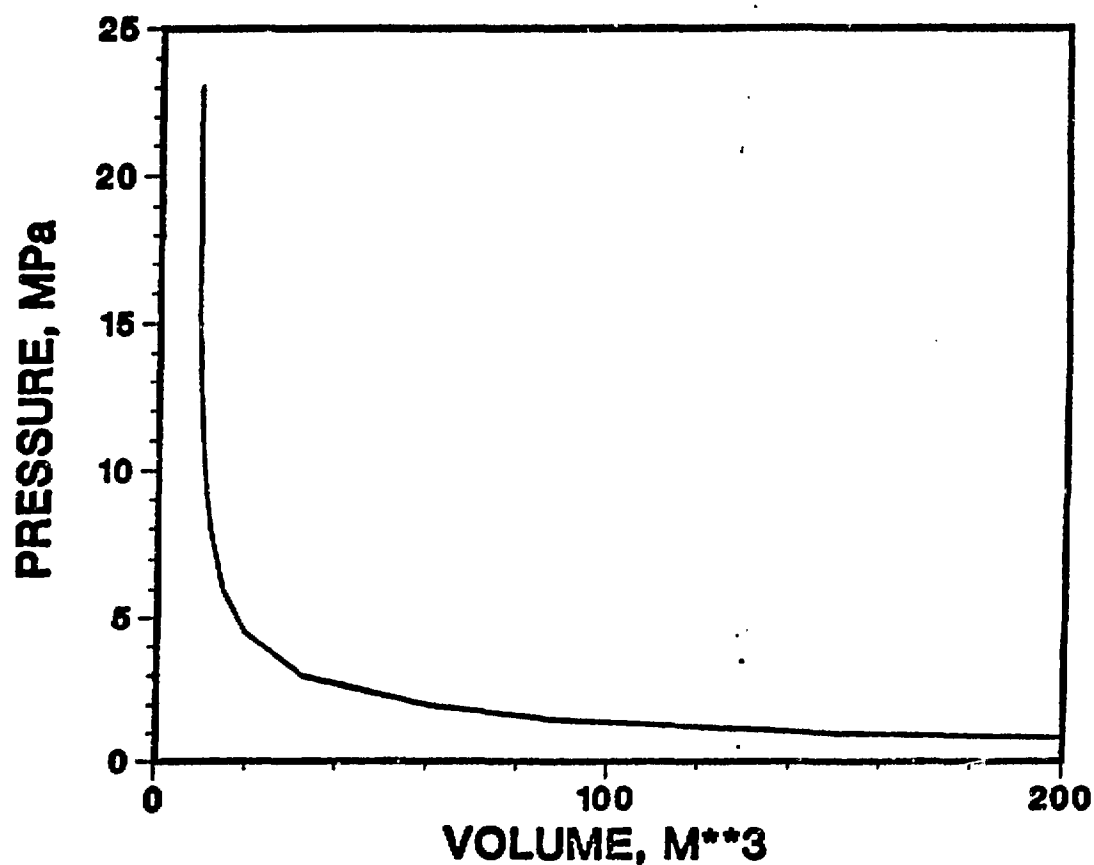


Fig. 3. Source Term for Core-Gas Bubble Used in ALICE-II Analysis

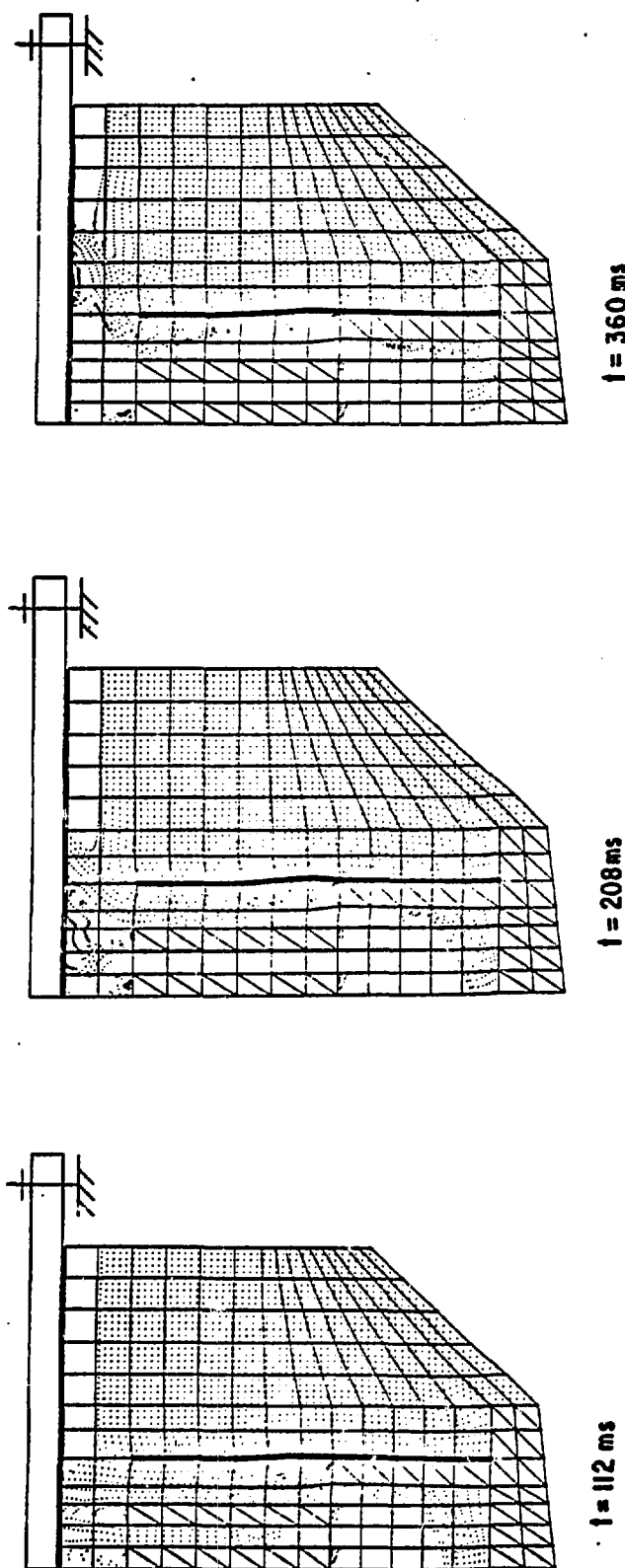


Fig. 4. Time Sequence of ALICE-III HCDA Calculations for Pool Reactor with Annular U1S

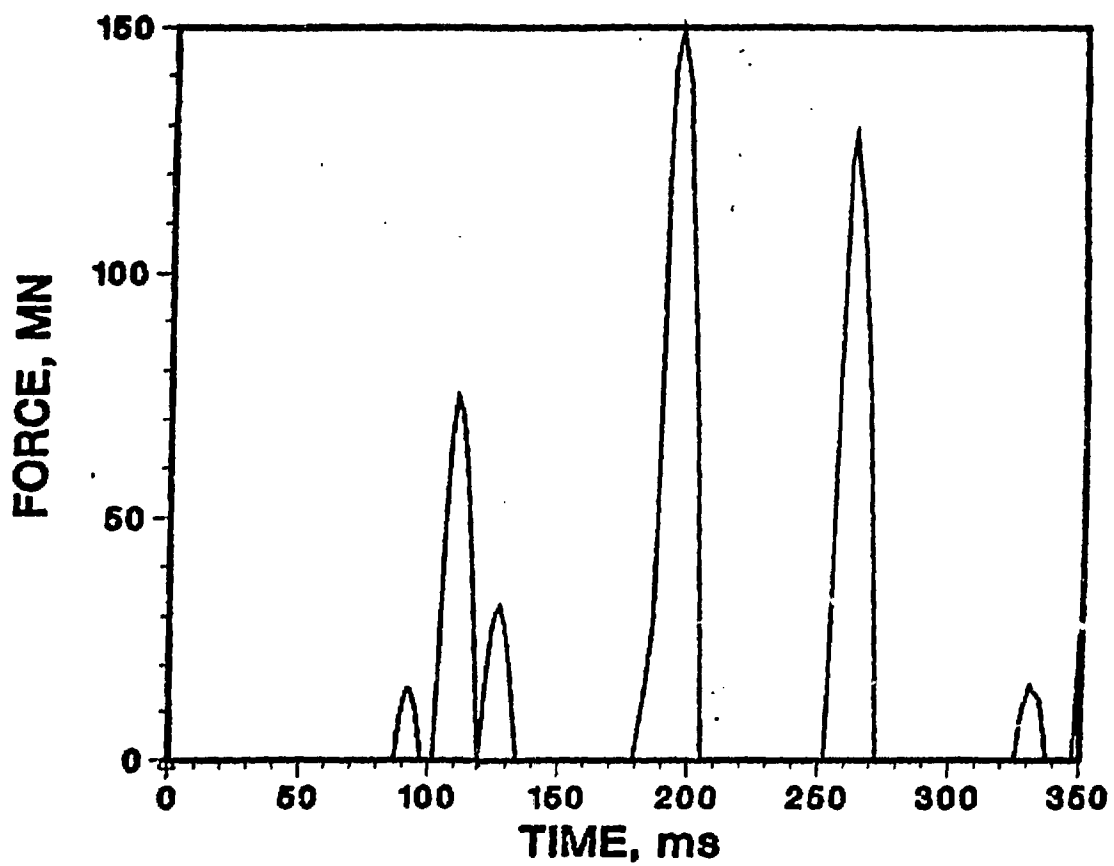


Fig. 5. Force History of Reactor Cover for Reference Case

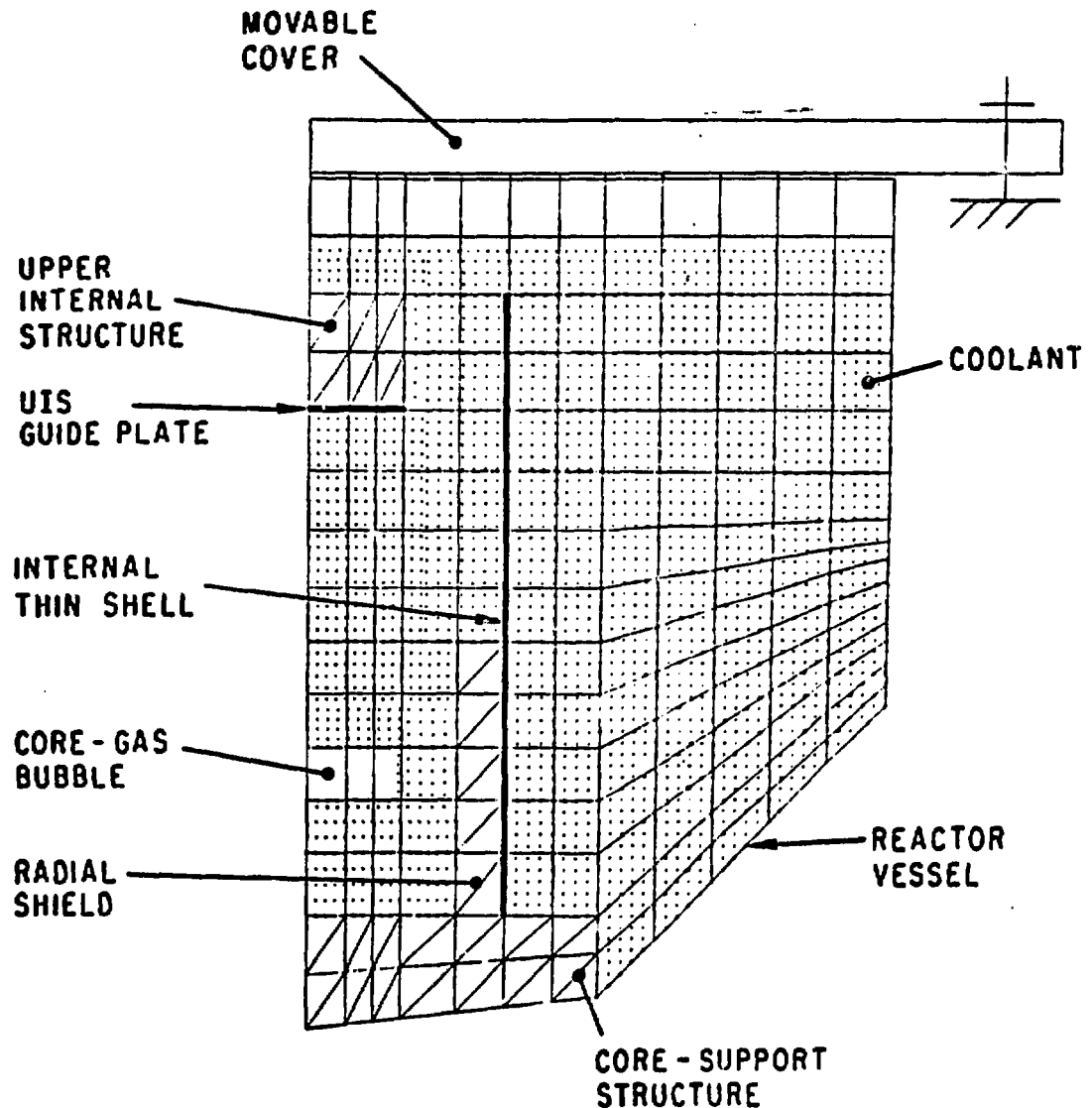
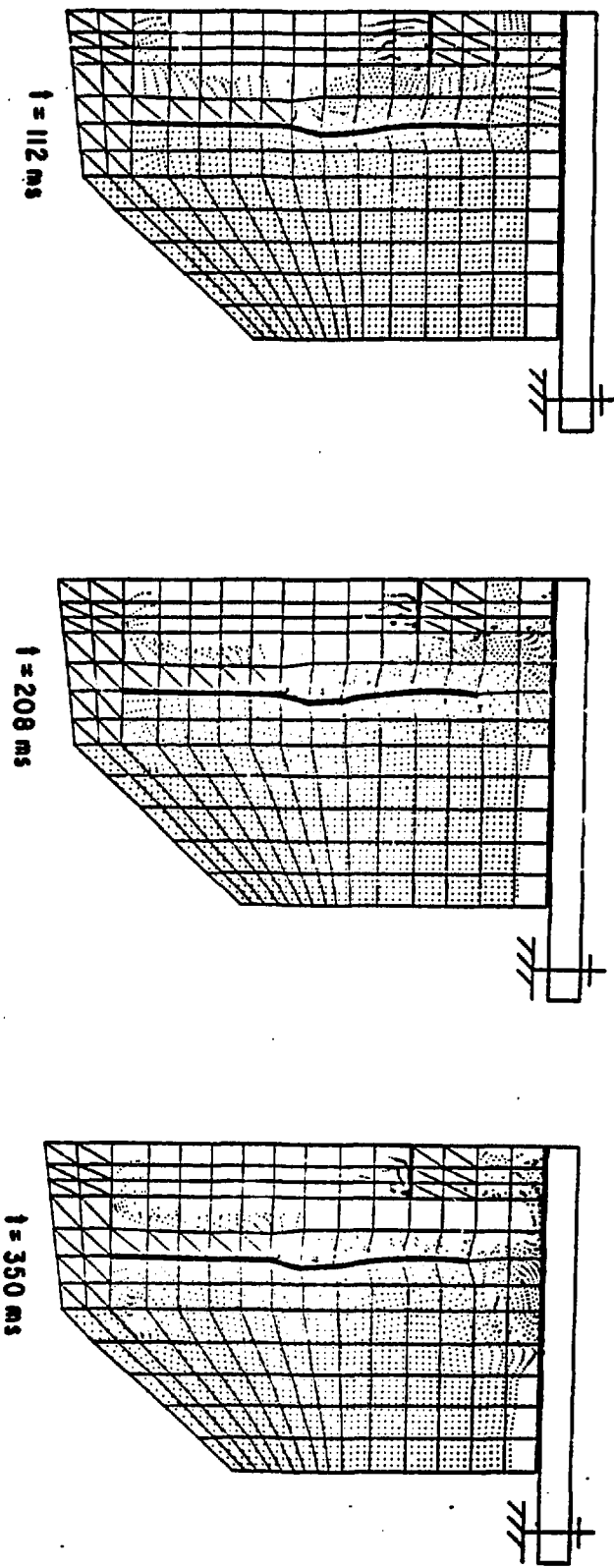


Fig. 6. ALICE-II Model of Pool Reactor with UIS Guide Plate

Fig. 7. Time Sequence of ALICE-II HCDA Calculations for Pool Reactor with UIs



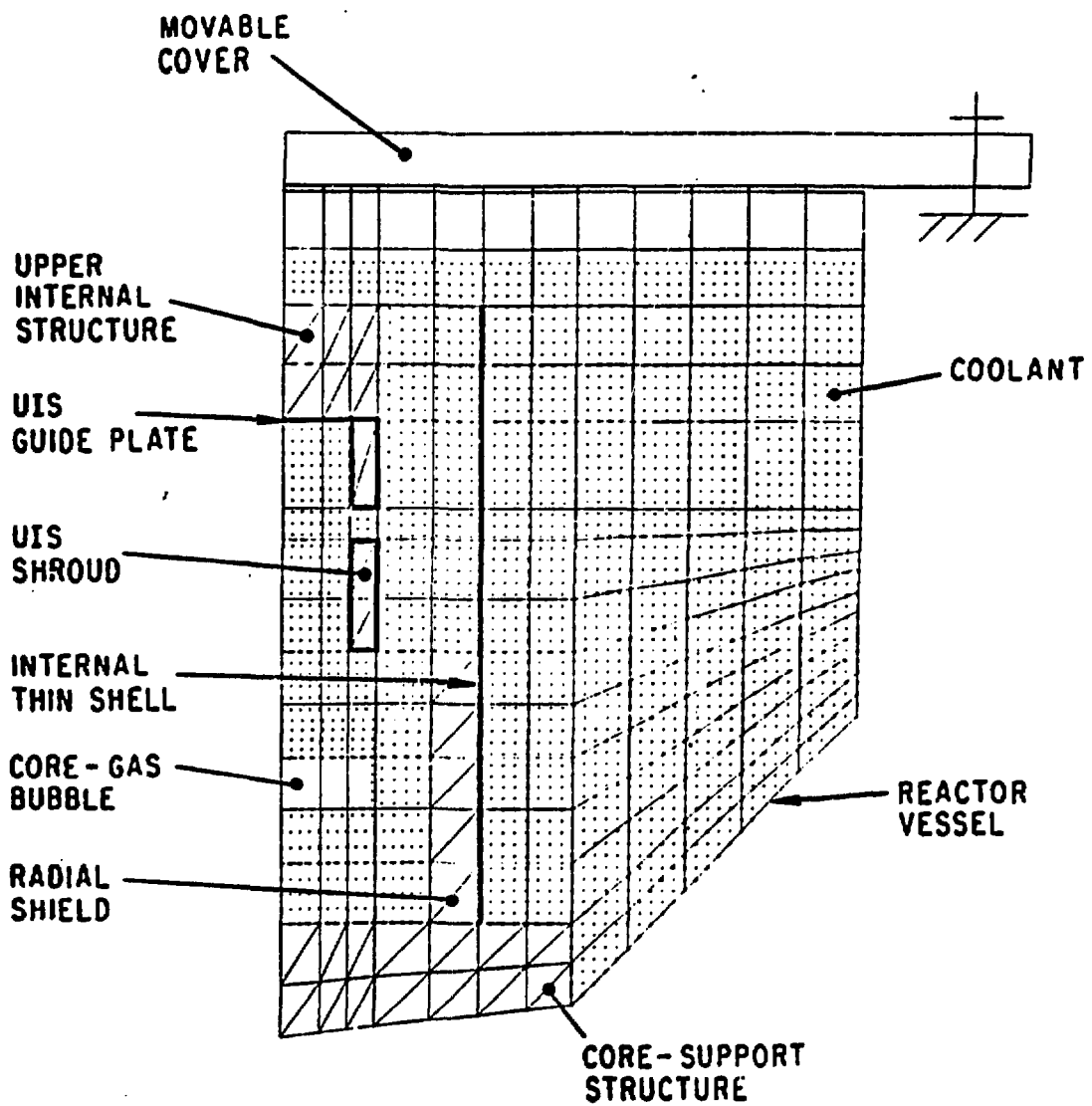


Fig. 8. ALICE-II Model of Pool Reactor with Guide Plate and UIS Shroud

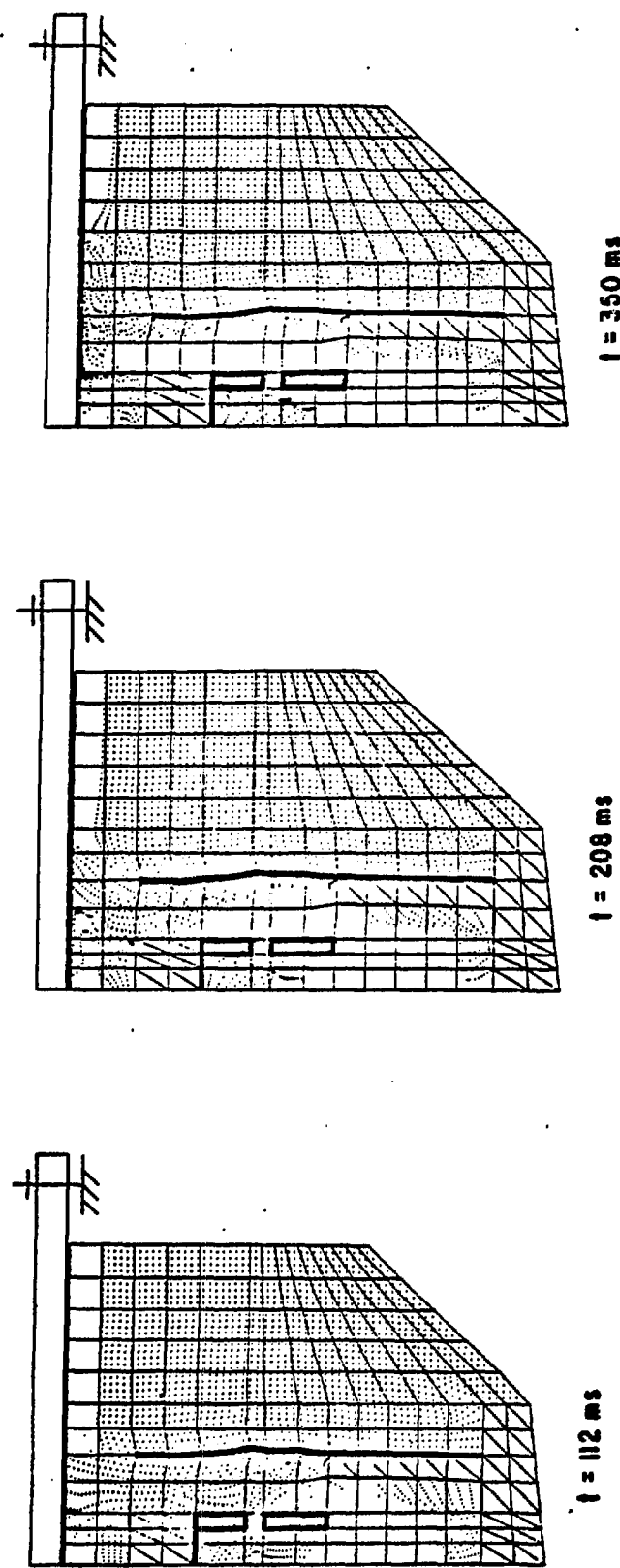
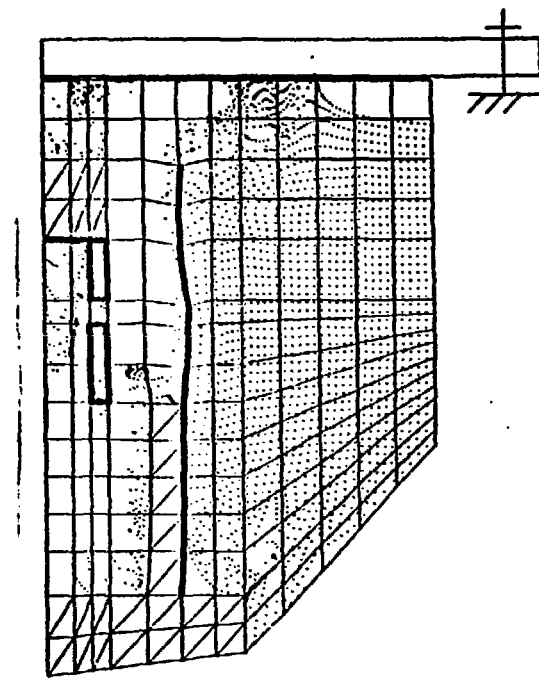
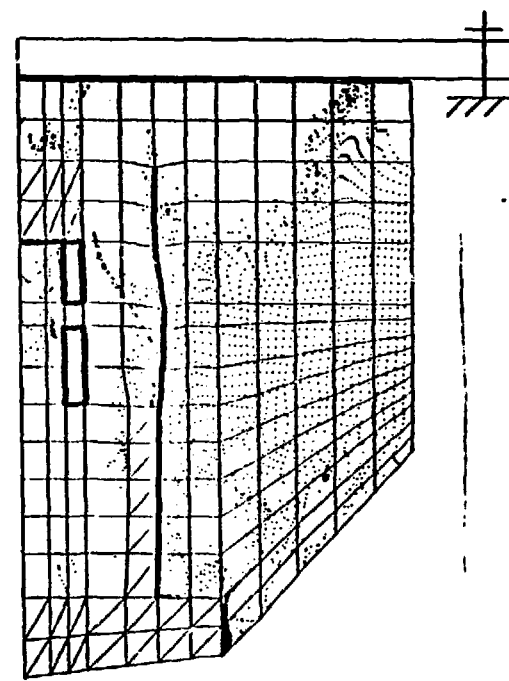


Fig. 9. Time Sequence of ALICE-II HCDA Calculations for Pool Reactor with Guide Plate and U1S Shroud



$t = 530 \text{ ms}$



$t = 1090 \text{ ms}$

Fig. 10. Time Sequence of ALICE-II HCDA Calculations for Pool Reactor with Guide Plate and UIS Shroud

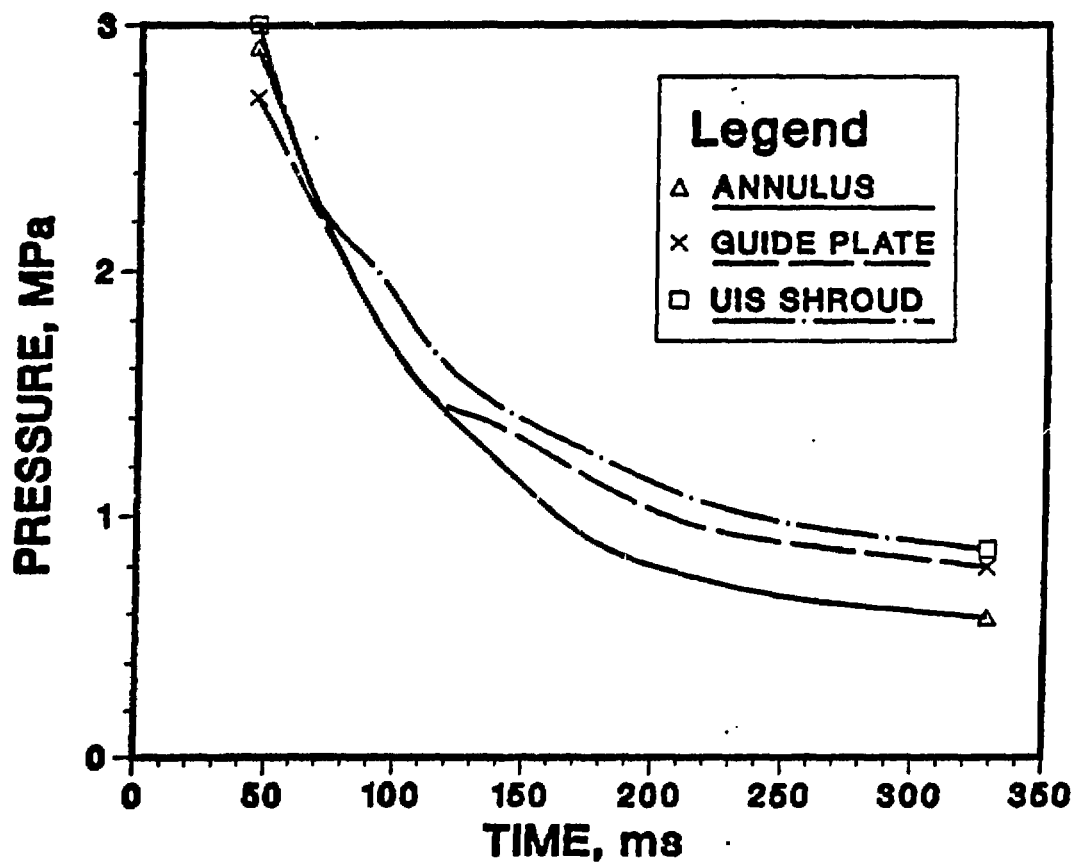


Fig. 11. A Comparison of Core Pressure Histories for the Three Cases

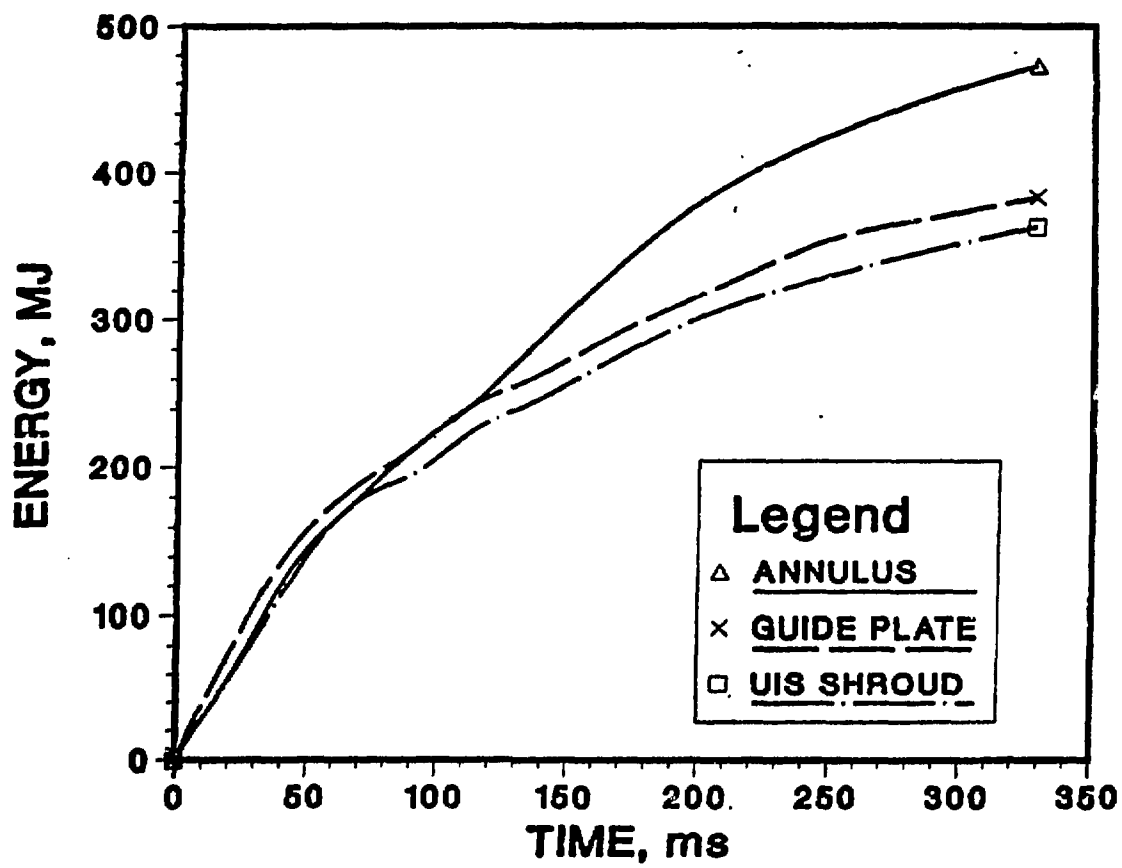


Fig. 12. A Comparison of Core Energy Released for the Three Cases